ATM- and ATR-Induced Primary Ciliogenesis Promotes Cisplatin Resistance in Pancreatic Ductal Adenocarcinoma

Yu-Ying Chao
National Cheng Kung University
Bu-Miin Huang
National Cheng Kung University
I-Chen Peng
National Cheng Kung University https://orcid.org/0000-0001-5826-500X
Yi-Shyun Lai
National Cheng Kung University
Wen-Tai Chiu
National Cheng Kung University https://orcid.org/0000-0003-0310-0675
Yi-Syuan Lin
National Cheng Kung University https://orcid.org/0000-0001-6574-6952
Shih-Chieh Lin
National Cheng Kung University https://orcid.org/0000-0002-9967-5037
Jung-Hsuan Chang
National Cheng Kung University
Pai-Sheng Chen
National Cheng Kung University https://orcid.org/0000-0003-0513-1467
Shaw-Jenq Tsai
National Cheng Kung University https://orcid.org/0000-0002-3569-5813
Chia-Yih Wang (b89609046@gmail.com)
National Cheng Kung University https://orcid.org/0000-0002-9196-0802

Research Article

Keywords: Chemoresistance, primary cilia, centriolar satellite, autophagy, ATM, ATR

Posted Date: December 2nd, 2021

DOI: https://doi.org/10.21203/rs.3.rs-942728/v1

Abstract

Background

Pancreatic ductal adenocarcinoma (PDAC) is one of the most lethal cancers because of its late diagnosis and chemoresistance. Primary cilia, the cellular antennae, are observed in most human cells to maintain development and differentiation. Primary cilia are gradually lost during the progression of pancreatic cancer and are eventually absent in PDAC. However, recent study showed that primary cilia regrowth contributes to the development of diverse kinase inhibitor resistance in lung cancer. We elucidated the role of regrowth primary ciliogenesis in PDAC chemoresistance and uncovered the underlying molecular mechanism.

Results

We showed that cisplatin-resistant PDAC regrew primary cilia. Additionally, genetic or pharmacological disruption of primary cilia sensitized PDAC to cisplatin treatment. Mechanistically, ataxia telangiectasia mutated (ATM) and ATM and RAD3-related (ATR), tumor suppressors that initiate DNA damage responses, promoted the excessive formation of centriolar satellites (EFoCS) and autophagy activation. Disruption of EFoCS and autophagy inhibited primary ciliogenesis, sensitizing PDAC cells to cisplatin treatment.

Conclusions

Collectively, our findings revealed an unexpected interplay among the DNA damage response, primary cilia, and chemoresistance in PDAC and deciphered the molecular mechanism by which ATM/ATR-mediated EFoCS and autophagy cooperatively regulate primary ciliogenesis.

Background

Pancreatic ductal adenocarcinoma (PDAC) is highly malignant with a poor prognosis [1, 2]. It is the most frequent type of pancreatic cancer, and more than 90% of patients with pancreatic cancer are diagnosed with PDAC. Lacking early symptoms, most PDAC patients are diagnosed at advanced disease stages, leading to a poor five-year survival rate of only 9%. Clinically, complete tumor resection, radiation therapy, and chemotherapy are commonly used to treat PDAC [3]. Despite the advances in chemotherapy, the poor prognosis of PDAC patients has not improved because of the rapid development of drug resistance. Thus, deciphering the molecular mechanism of developing drug resistance is an essential issue to improve the clinical outcome during PDAC treatment.

Most chemotherapies eliminate cancer cells by directly or indirectly targeting DNA. In response to DNA damage, cells coordinate a series of signaling pathways to detect and repair DNA lesions, termed the DNA damage response [4, 5]. Ataxia telangiectasia mutated (ATM), ATM-Rad3-related (ATR) and DNA-dependent protein kinase (DNA-PK), members of the phosphatidylinositol 3-kinase-related protein kinase

(PI3KK) superfamily, initiate the DNA damage response for cell cycle arrest, damage repair, or even apoptosis when damage is irreversible. Although ATM and ATR are long considered tumor suppressors, inhibition of ATM or ATR signaling ameliorates drug sensitivity, particularly in radioresistant and chemoresistant cancer cells [6, 7]. Thus, ATM and ATR inhibitors have been developed to improve chemotherapeutic efficiency in cancer therapy [8, 9].

Primary cilia are detected in most human cells; they are cellular antennae responsible for receiving and transducing environmental signals into cells. Thus, precise regulation of primary cilia is required for proper development and differentiation [10-13]. Loss of primary cilia occurs in the early stage of oncogenic transformation and tumorigenesis [14, 15]. During the development of pancreatic tumors, the numbers of primary cilia decrease gradually from normal pancreatic ductal epithelium to pancreatic intraepithelial neoplasia (PanIN) [16]. Eventually, cilia are scarcely detected in PDAC. Although the loss of primary cilia is one of the hallmarks of PDAC, a recent study showed that the regrowth of primary cilia contributes to the development of diverse kinase inhibitor resistance in lung cancer [17]. Thus, primary cilia may play a role in modulating drug resistance.

Centriolar satellites are nonmembranous, electron-dense granules scattered around centrosomes. Because of a substantial overlap between the protein compositions and functions of satellites with centrosomes and cilia, centriolar satellites are considered parts of the centrosome or cilium complexes [18]. Pericentriolar material-1 (PCM1) acts as a scaffold protein to organize other components of satellites [19]. Centriolar satellites are moved dynamically along the microtubules by the dynein/dynactin complex. Following DNA damage, excessive formation of centriolar satellites (EFoCS) around centrosomes induces centrosome amplification [20]. Additionally, removing several components, such as CEP131, CEP290, and PCM1, from centriolar satellites promotes primary ciliogenesis [21]. However, the depletion of several centriolar satellite genes inhibits primary ciliogenesis [19, 22]. Thus, the proper dynamics of centriolar satellites maintain primary ciliogenesis.

Autophagy is also linked to primary cilia formation. Inhibition of autophagy alleviates serum deprivation-induced primary cilia. Additionally, autophagy participates in chemotherapeutic resistance [23]. Autophagy maintains energy homeostasis by degrading and recycling macromolecules. During metabolic stress, AMP-activated protein kinase (AMPK) and UNC-51-like kinase-1 (ULK1) are activated for autophagy initiation [24]. ATG7-mediated lipidation of LC3 promotes the conversion of LC3-I to LC3-II for autophagosome formation [25]. After fusion with lysosomes, autolysosomes are formed, followed by degradation of the contents of autophagosomes. Although autophagy has been studied extensively, the interplay among the DNA damage response, autophagy, and chemoresistance is unclear.

PDAC cells were devoid of primary cilia. Here, we showed that following chemotherapeutic drug treatment, PDAC cells regrew primary cilia, leading to chemoresistance. Mechanistically, ATM and ATR induced EFoCS and activated autophagy, two events that cooperatively contributed to primary ciliogenesis. Thus, we have uncovered the novel function and underlying molecular mechanism by which primary cilia contribute to the development of chemoresistance in pancreatic ductal adenocarcinoma.

Results

Primary cilia contribute to cisplatin resistance in PDAC.

Primary cilia contribute to kinase inhibitor resistance in lung cancer; however, the underlying molecular mechanism remains unclear. Loss of primary cilia was observed in pancreatic ductal adenocarcinoma (PDAC); thus, we investigated whether primary cilia contribute to chemoresistance in PDAC and how primary ciliogenesis is regulated. To test our hypothesis, PANC-1 cells were treated with several chemotherapeutic drugs, and primary cilia were examined. Primary cilia were scarcely observed in PANC-1 cells. However, when cells were treated with cisplatin (CPT), gemcitabine (GEM), and etoposide (ETO), the proportion of cells with primary cilia increased, while paclitaxel (Taxol) did not affect primary ciliogenesis (Figs. 1A-B and S1A-B). Additionally, the cells grew primary cilia in a dose- and time-dependent manner (Figs. 1C-E and S2A-C). A marker of ciliary axoneme, acetylated tubulin, was also increased following CPT and GEM treatment (Figs. 1F and S2D), suggesting that chemotherapeutic drugs induced primary cilia formation. The expression of ciliary genes, including KIF7, SCLT1, IFT43, RNF38, TOPORS, and C5orf30, increased significantly following CPT, GEM, and ETO treatment (Fig. S3A-C). The structure of the primary cilium was further examined in detail by immunofluorescence staining. CEP164 (a distal appendage marker; Fig. 1G), acetylated tubulin (an axoneme marker; Fig. 1G-I), ARL13b (a ciliary membrane marker; Fig. 1H), and IFT88 (an intraflagellar transporter marker; Fig. 1I) were detected in CPT-induced primary cilia, suggesting that these cilia contained essential ciliary components. Next, we tested whether CPT-resistant PANC-1 cells grew primary cilia. In parental cells, seeding cells at a low density of $5x10^4$ did not induce primary ciliogenesis following CPT treatment, and the ability of PANC-1 cells to grow primary cilia increased in a density-dependent manner (Fig. 1J). Importantly, CPT-resistant PANC-1 cells at a density of $5x10^4$ grew primary cilia (Fig. 1K), and these cilia contained essential ciliary components (Fig. S4A-C). Thus, chemoresistant PANC-1 cells grew primary cilia.

Next, we tested whether primary cilia contributed to chemoresistance in PANC-1 cells. PANC-1 cells were transfected with siRNA against IFT88 for 72 h, followed by the examination of primary cilia and cell viability. The IFT88 abundance was reduced efficiently (Fig. 2A), and IFT88 depletion inhibited CPT- or GEM-induced primary ciliogenesis (Figs. 2B and S5A). We then examined the role of primary cilia in chemoresistance. IFT88 knockdown did not affect cell viability but sensitized cells to CPT or GEM treatment (Figs. 2C-D and S5B-C). Importantly, IFT88 depletion reduced cell viability in CPT-resistant PANC-1 cells (Fig. 2E). To further confirm this finding, five different shRNA sequences against IFT88 (shIFT88#1-5) were delivered into cells by lentivirus infection. All five sequences reduced IFT88 expression, and shIFT88#3 had the highest knockdown efficiency (Fig. S5D). IFT88 depletion with shIFT88#3 reduced primary ciliogenesis (Fig. S5E) and sensitized cells to either CPT or GEM treatment (Fig. S5F-H). This finding was further strengthened by treating cells with roscovitine, a known primary cilia inhibitor [26]. Following CPT or GEM treatment, roscovitine efficiently alleviated primary cilia formation (Figs. 2F and S5I). Additionally, roscovitine sensitized cells to CPT treatment (Figs. 2G) and reduced cell viability in CPT-resistant PANC-1 cells (Fig. 2H). The data suggest that primary cilia contribute to chemotherapeutic resistance in PANC-1 cells.

Next, the initiation of primary ciliogenesis was examined. Removal of CP110 from the distal end of the mother centriole initiates primary ciliogenesis following serum starvation [27]. Typically, two CP110 proteins cap the distal ends of both mother and daughter centrioles (Fig. S6A), and CP110 was displaced from the mother centriole for ciliogenesis during serum starvation (Fig. S6B). Interestingly, following CPT treatment, CP110 was removed from the mother centriole for ciliogenesis, but several CP110-aggregated puncta were scattered around the primary cilia (Fig. S6C). The data suggest that CP110 removal for ciliogenesis is triggered by serum starvation and CPT treatment; however, aberrant accumulation of CP110 around the cilia occurs in CPT-treated PANC-1 cells.

Excessive formation of centriolar satellites contribute to primary ciliogenesis.

Centriolar satellites dynamics regulate primary cilia formation; thus, the centriolar satellites were examined. Typically, centriolar satellites are scattered around the centrosomes; however, excessive formation of centriolar satellites (EFoCS) occurred following CPT treatment, as shown by several centriolar satellite markers: PCM1 (Figs. 3A-B and S7A; supplementary video 1-2), OFD1 (Fig. S7B-C), and BBS4 (Fig. S7D-E). Interestingly, the amount of centriolar satellite scaffold PCM1 was upregulated following CPT treatment (Fig. 3C). We next tested whether EFoCS contributed to primary cilia formation and chemoresistance. PCM1 was depleted by siRNA transfection (Figs. 3D and S7F), and PCM1 depletion alleviated CPT-induced primary cilia (Fig. 3E). Importantly, PCM1 knockdown had a modest effect on cell viability but sensitized cells to CPT treatment (Fig. 3F-G). Additionally, PCM-1 depletion reduced cell viability in CPT-resistant PANC-1 cells (Fig. 3H). The data suggest that excessive formation of centriolar satellites contributes to primary ciliogenesis and chemoresistance. To further confirm this finding, EFoCS was disrupted by depleting $p150^{glued}$, a key component of the dynein/dynactin complex for regulating centriolar satellite movement [28]. $p150^{glued}$ depletion efficiently disrupted EFoCS and inhibited primary cilia formation, supporting excessive formation of centriolar satellites led to primary cilia formation (Fig. 3I-K). Furthermore, EFoCS was disrupted by treating cells with sodium orthovanadate [20]. Sodium orthovanadate efficiently alleviated primary ciliogenesis and sensitized cells to CPT or GEM treatment (Fig. S7G-J). Taken together, excessive formation of centriolar satellites induces primary ciliogenesis for chemoresistance.

ATM and ATR contribute to primary ciliogenesis for cisplatin resistance.

Genotoxic stresses contribute to primary cilia formation via the DNA damage response in retinal pigmented epithelium [29]. Next, we tested whether the DNA damage response participated in primary ciliogenesis and chemoresistance in PANC-1 cells. CPT induced DNA damage, as shown by increased γ-H2AX (Figs. 4A and S8A). The DNA damage responses were then examined. CPT activated DNA damage signaling, including ATM, ATR, and DNA-PK (Figs. 4B). Depletion of ATM and ATR by transfecting cells with specific siRNA alleviated CPT-induced primary cilia formation (Fig. 4C-F). However, depletion of DNA-PK did not affect CPT-induced primary ciliogenesis (Fig. S8B-C). Thus, we checked the effect of ATM and ATR on the chemosensitivity of PANC-1 cells. Depletion of either ATM or ATR had modest or no effects on cell viability but sensitized cells to CPT treatment (Fig. 4G-J). Inhibition of ATM by its selective inhibitor

Ku55933 also sensitized cells to CPT treatment (Fig. S8D). Importantly, depletion of ATM or ATR reduced cell viability in CPT-resistant PANC-1 cells (Fig. 4K). This finding was further confirmed by treating CPT-resistant PANC-1 cells with ATM and ATR inhibitors (Fig. S8E). Thus, ATM- and ATR-induced primary cilia contribute to chemoresistance in PANC-1 cells.

The downstream effectors were then examined. CHEK1, CHEK2, AKT, and p53 were activated following CPT treatment (Fig. 5A-D). We then examined whether activation of these effectors contributed to primary ciliogenesis. Inhibition of CHEK1 and p53 did not affect CPT-induced ciliogenesis (Fig. S9A-B); however, CPT-induced primary cilia were reduced significantly when CHEK2 and AKT were inactivated (Fig. S9C-D). To further confirm these findings, the effectors were depleted by specific siRNA and then primary ciliogenesis was examined. Surprisingly, the depletion of CHEK1, CHEK2, or AKT did not inhibit CPT-induced primary ciliogenesis (Fig. 5E-J), implying that other signaling pathways may play important roles in triggering primary cilia formation following CPT treatment.

Autophagy contributes to primary ciliogenesis.

Autophagy contributes to primary cilia formation [29, 30]. Thus, we speculated whether autophagy contributed to CPT-induced primary ciliogenesis. CPT treatment activated autophagy, as evidenced by increased LC3 puncta (Fig. 6A) and the LC3 II to I ratio (Fig. 6B). To further confirm this finding, the initiation of autophagy was examined. Increased phosphorylation of AMPK at Thr172 (active site) and decreased phosphorylation of ULK1 at Ser757 (inhibitory site) were observed following CPT treatment (Fig. 6C-D). Pharmacological inhibition of autophagy by treating cells with chloroquine (CQ), bafilomycin A1 (BafA1), or ULK1 inhibitor (ULK1i) alleviated primary cilia formation, implying that autophagy contributed to ciliogenesis (Fig. S10A-C). To further confirm our finding, ATG7 was depleted by infecting cells with lentivirus containing different shRNA sequences against ATG7. ATG7 was efficiently depleted by shATG7#3 (Fig. 6E), and CPT-induced ciliogenesis was reduced significantly in ATG7-deficient cells (Fig. 6F). ATG7 depletion had no effect on cell viability but sensitized cells to CPT treatment (Fig. 6G-H), and this finding was further supported by treating cells with chloroquine (Fig. S10D). Furthermore, treating cells with AMPK or ULK1 inhibitor reduced cell viability in CPT-resistant PANC-1 cells (Fig. 6I). Thus, autophagy promotes CPT resistance in PANC-1 cells.

Next, we examined whether ATM and ATR regulated primary ciliogenesis and chemoresistance via autophagy and excessive formation of centriolar satellites. Depletion of ATM or ATR alleviated CPT-induced AMPK activation, suggesting that autophagy was regulated by ATM and ATR activation (Fig. 7A-B). Next, we examined the excessive formation of centriolar satellites, which was reduced in ATM- or ATR-deficient cells (Fig. 7C-D). Additionally, the depletion of ATM or ATR also reduced the levels of CPT-increased PCM1 (Fig. 7E), and these data were further supported by treating cells with caffeine, a PI3KK paninhibitor (Fig. 7F). Taken together, ATM and ATR trigger excessive formation of centriolar satellites and autophagy cooperatively for primary ciliogenesis, leading to chemoresistance.

Discussion

PDAC cells were devoid of primary cilia. Here, we showed that following chemotherapeutic drug treatment, PDAC cells regrew primary cilia. We uncovered the novel function of ATM and ATR in regulating primary cilia formation, at least partly contributing to cisplatin resistance in PDAC. We further demonstrated that activated ATM and ATR promoted primary ciliogenesis via excessive formation of centriolar satellites (EFoCS) and autophagy (Fig. S11). Thus, our study unraveled the interplay among the DNA damage response, primary cilia, and chemoresistance.

Most cells in our body grow primary cilia. However, the loss of primary cilia has been observed during tumorigenesis, including colon, breast, and pancreatic cancers [14, 31, 32]. Surprisingly, recent studies have shown that primary cilia are linked to chemoresistance in lung and breast cancers. During the development of diverse kinase inhibitor resistance in lung cancer, primary cilia can regrow [17]. Additionally, sonic hedgehog signaling facilitates the stemness of mammary tumor-initiating cells via primary cilia [33]. Thus, when cancer cells develop more malignant chemoresistance and stemness phenotypes, primary cilia reappear. In our study, cisplatin-resistant PDAC cells grew primary cilia. Importantly, genetic or pharmacological disruption of these cilia sensitized resistant PDAC cells to cisplatin treatment, supporting that primary cilia contributed to chemoresistance. It remains unclear how primary cilia contribute to chemoresistance. Previous study showed that primary cilia maintained DNA damage responses when exposing to genotoxic stresses [34]. DNA damage responses maintain cell survival and genome integrity by repairing damaged genome [4]. We that speculated that primary cilia accelerated DNA damage responses to maintain cell survival and repair damaged DNA in CPT-resistant PANC-1 cells. Disruption of primary cilia attenuated DNA damage response, leading to robust DNA damage and sensitizing cells to cisplatin. Thus, our study strengthened the role of primary cilia in contributing to the development of chemoresistance in pancreatic cancers. Investigating whether these cilia-harboring cells show stemness and what signaling pathway contributes to these events will be important issues in the future.

ATM and ATR are tumor suppressors that maintain genome integrity by regulating DNA damage responses [35]. In addition to acting on the damaged genome, ATM and ATR are also correlated with chemoresistance. For example, ATM is hyperactivated following chemotherapy, thus maximizing the DNA damage response to maintain the survival of drug-resistant leukemic cells [36]. Additionally, ATM-dependent activation of transglutaminase 2 and NF-κB signaling promotes a doxorubicin-resistant phenotype in breast cancers. Interestingly, using 3D-reconstituted basement membrane breast and lung cancer cell culture models, ATR is activated, promoting cisplatin resistance by activating translesion DNA synthesis modulation. Furthermore, in high-grade serous ovarian cancer, multiple resistance mechanisms to cisplatin have been revealed [37]. However, inhibition of PARP and ATR simultaneously increased DNA damage and sensitized high-grade serous ovarian cancer cells to chemotherapy [34]. Thus, targeting ATM and ATR is considered a novel approach to overcome drug resistance. In our study, we also demonstrated that activation of ATM and ATR contributed to cisplatin resistance in PDAC. Aside from their canonical roles in maintaining genome integrity, we showed that ATM and ATR promoted cisplatin resistance, at least partly by inducing primary ciliogenesis. Either ATM- or ATR-mediated nuclear or ciliary events

cooperatively contribute to chemoresistance in PDAC. Thus, targeting the inhibition of ATM and ATR can be used as adjuvant therapy to offer clinically important distinctions in treating patients with PDAC.

Centriolar satellites are associated with primary ciliogenesis. Orofaciodigital syndrome type I (OFD1), a component of centriolar satellites, is removed from centriolar satellites by autophagy for primary cilia formation during serum starvation [38]. However, following etoposide treatment, OFD1 is displaced from centriolar satellites, and inhibition of autophagy does not reverse this phenotype, suggesting that etoposide-induced OFD1 removal is independent of autophagy [29]. Additionally, in response to other cellular stresses, such as UV radiation, heat shock, and transcription stresses, p38 is activated, displacing PCM1, AZI1, and CEP290 from centriolar satellites for primary cilia formation [21]. These data suggest that the displacement or degradation of centriolar satellite components promotes primary cilia formation following metabolic or genomic stresses. However, excessive formation of centriolar satellites (EFoCS) has been observed in response to DNA damage, and EFoCS is required to induce centrosome amplification [20]. Thus, under different cellular stresses, some components of centriolar satellites may displace from or aggregate to centriolar satellites around the centrosome/basal body. Here, we showed that in PDAC, cisplatin induced primary ciliogenesis and EFoCS. Importantly, PCM1, a centriolar satellite scaffold, was also upregulated. Depletion of PCM1 inhibited primary ciliogenesis. More importantly, the disruption of dynactin to suppress EFoCS alleviated cisplatin-induced primary cilia, suggesting that EFoCS contributed to primary cilia formation. Thus, different cellular stresses lead to distinct centriolar satellite dynamics for primary cilia formation. How centriolar satellite dynamics affect primary cilia remains unclear. Centriolar satellites are required for primary cilia because the depletion of several satellite components inhibits primary ciliogenesis. However, following metabolic or genomic stresses, primary cilia grew, but disruption of centriolar satellites was observed, suggesting that the role of centriolar satellites in primary ciliogenesis is stress dependent. How centriolar satellite dynamics affect primary cilia formation must be clarified in the future.

Conclusion

In this study, we uncovered the novel role of ATM and ATR in cisplatin resistance in PDAC, at least partly by inducing primary cilia formation. ATM- and ATR-induced EFoCS and autophagy cooperatively promote primary cilia. Thus, ATM and ATR not only prevent cancer cell death by maintaining genome integrity but also facilitate primary cilia, leading to cisplatin resistance in PDAC.

Methods

Cell culture

The human pancreatic ductal adenocarcinoma (PANC-1) cell line was maintained in Roswell Park Memorial Institute (RPMI)-1640 medium containing 10% fetal bovine serum (FBS) and 1% sodium pyruvate. Stable knockdown of IFT88 (shIFT88#3) was generated in PANC-1 cells via the lentiviral delivery of shRNA against IFT88 (#3; clone TRCN0000141713; RNAi core lab of Genomics Research

Center, Academia Sinica, Taipei, Taiwan). Stable cells were selected with puromycin (1 μg/ml).
To establish cisplatin-resistant pancreatic cancer cells, PANC1 cells were initially treated with a low dose of cisplatin (0.5 μM) for one month and then the dose of cisplatin was gradually increased to 1, 2 and 4 μM (each dose for one month of incubation). The culture medium of RPMI-1640 with cisplatin was changed every two days. CPT-resistant PANC-1 cells were maintained in 4 μM cisplatin-containing culture medium. All the cell lines were cultured at 37 °C in a humidified atmosphere of 5% CO_2. These cells were regularly examined for mycoplasma contamination by immunofluorescence staining and immunoblotting assays according to published methods [39].

Drug treatments

Cisplatin (CPT; 232120; 5 μM), gemcitabine (GEM; G6423; 100 μM), etoposide (ETO; E1383; 100 μM), hydroxyurea (HU; H8627; 1 mM), paclitaxel (Taxol; T7402; 0.1 μg/ml), roscovitine (Rosco; R7772; 20 μM), Ku55933 (ATMi; SML1109; 10 μM), Akt inhibitor IV (Akti; 124011; 5 μM), p53 inhibitor (p53i; pifithrin-α; 506170; 10 μM), Chk1 inhibitor (Chk1i; UCN-01; 10 μM), Chk2 inhibitor II (Chk2i; 220486; 10 μM), caffeine (C0750; 2 mM), sodium orthovanadate (SOV; S6508; 1 μM) and SBI-0206965 (ULK1i; SML1540; 10 μM) were purchased from Sigma, St. Louis, MO. Berzosertib (ATRi; VE-822; 100 nM) and dorsomorphin (AMPKi; S7306; 5 μM) were purchased from Selleck Chemicals, Houston, USA. Bafilomycin-A1 (Baf. A1; 196000; 10 nM) was purchased from Enzo, NY, USA. Chloroquine (CQ; NBP2-29386; 100 μM) was purchased from Novus Biologicals (Littleton, CO, USA).

Antibodies

The following antibodies were obtained commercially:

Anti-Ku70 (N3H10; GTX23114), anti-Ku80 (GTX109935), anti-ATM (2C1; GTX70103), anti-ATR (GTX128146), anti-β-actin (AC-15; GTX26276), anti-β-tubulin (GTX101279), anti-DNA-PKcs (phospho-Thr2609; GTX24194), anti-p53 (DO1; GTX70214), anti-Akt (phospho-Ser473; GTX128414), and anti-p53 (GTX70214) were purchased from GeneTex (Irvine, CA); anti-acetylated-tubulin (T6793), anti-γ-tubulin (T6557), and anti-ATG7 (A2856) were purchased from Sigma (St. Louis, MO); anti-ATM (phospho-Ser1981; ab81292), anti-CP110 (ab99338), and anti-BBS4 (ab197122) were purchased from Abcam (Cambridge, UK); anti-IFT88 (13967-1-AP), anti-ARL13B (17711-1-AP), and anti-AZI1 (25735-1-AP) were purchased from Proteintech (Chicago, IL); anti-ULK1 (phospho-Ser757; #6888), anti-ULK1 (D8H5; #8054), anti-AMPK (phospho-Thr172; 40H9; #2535), anti-AMPK (#2532), anti-ATR (phospho-Ser428; #2853), anti-LC3A/B (D3U4C) XP (#12741), anti-PCM1 (Q15; #5259), anti-Chk2 (phospho-Thr68; #2661), anti-Chk2 (#3440), anti-Akt (phospho-Ser473; #4060), anti-Akt (#4691), anti-p44/42 MAPK (Erk1/2; phospho-Thr202/Tyr204; #4370), anti-p44/42 MAPK (Erk1/2; #4695), anti-p53 (phospho-Ser15; #9284), anti-Chk1 (phospho-Ser317; #12302), and anti-Chk1 (#2360) were purchased from Cell Signaling (Beverly, MA, USA); anti-OFD1 (NBP1-89355) and anti-CEP164 (NBP1-81445) were purchased from Novus (Littleton, CO); anti-$p150^{glued}$ (610473) was purchased from BD Biosciences, Mississauga, ON, Canada.

Immunofluorescence microscopy

Cells were fixed with ice-cold methanol at −20 °C for 5 min. After washing with PBS, the cells were blocked with 5% BSA for 1 hour at room temperature, followed by incubation with primary antibodies at 4 °C for 12 hours. Next, the cells were washed with PBS three times. After that, the cells were incubated with fluorescein isothiocyanate-conjugated or Cy3-conjugated secondary antibodies at room temperature for one hour in the dark. The nuclei were stained with 6-diamino-2-phenylindole (DAPI; 0.1 μg/ml) simultaneously. After washing with PBS three times, the coverslips were overlaid and mounted on glass slides in 50% glycerol. Prepared cells were observed using an Axio imager M2 fluorescence microscope (Zeiss, Switzerland) and captured using ZEN pro software (Zeiss, Switzerland). 3D images of excessive formation of centriolar satellites were generated using Imaris software (Zurich, Switzerland).

RNA interference (RNAi)

IFT88, CEP164, PCM1, $p150^{glued}$, ATM, ATR, DNA-PKcs, CHEK1, CHEK2 and AKT were depleted in human PANC-1 and cisplatin-resistant PANC-1 cells using annealed siRNAs with the following target sequences:

siIFT88: 5'-cgacuaagugccagacucauu [dt] [dt]-3' [40]

siCEP164: 5'-caggugacauuuacuauuuca [dt] [dt]-3' [41]

siPCM1: 5'-ggcuuuaacuaauuaugga [dt] [dt]-3' [42]

sip150: 5'-gccuugaacaguuccauca [dt] [dt]-3' [43]

siATM: 5'-aacauacuacucaaagacauu [dt] [dt]-3' [44]

siATR: 5'-aaccuccgugauguugcuuga [dt] [dt]-3' [44]

siDNA-PKcs: 5'-gggcgcuaaucguacugaa [dt] [dt]-3' [45]

siCHEK1: 5'-ucgugagcguuuguugaac-[dt][dt]-3' [46]

siCHEK2: 5'-aagaaccugaggaccaagaac [dt] [dt]-3' [46]

siAKT: commercially available from Cell Signaling (Cell Signaling Technologies; #6211)

Scrambled siRNA: 5'-gaucauacgugcgaucaga [dt] [dt]-3' (Sigma, St. Louis, MO).

For siRNA transfection, 6 μl of Lipofectamine 2000 (Invitrogen, Carlsbad, CA, USA) was mixed with 500 μl of Opti-MEM (Life Technologies, Grand Island, NY) for 5 min and then 2 μl of siRNA (100 μM in stock) in 500 μl of Opti-MEM was added to this mixture, which was then incubated at room temperature for 20 min before being layered onto cells in 1 ml of RPMI-1640 (100 nM working concentration). PANC-1 cells were harvested for further Experiments 72 h after transfection.

For shRNA transfection, lentiviruses were transfected into PANC-1 cells via the lentiviral delivery of three different anti-ATG7 shRNAs:

ATG7#1: TRCN0000007584, GCCTGCTGAGGAGCTCTCCAT

ATG7#2: TRCN0000007586, GCTTTGGGATTTGACACATTT

ATG7#3: TRCN0000007587, CCCAGCTATTGGAACACTGTA

All the lentiviruses were purchased from the RNAi core lab of Genomics Research Center, Academia Sinica, Taipei, Taiwan.

Quantitative Reverse Transcription PCR

RNA samples were extracted from the cultures using TRIzol Reagent (Invitrogen, Carlsbad, CA, USA). Reverse transcription was performed using the high-capacity cDNA Reverse Transcription Kit (Applied Biosystems, Waltham, MA) using 2 μg of total RNA. The resulting cDNA was used for real-time quantitative PCR (qPCR) using Fast SYBR Green Master Mix (Applied Biosystems, Waltham, MA) and StepOnePlus (Applied Biosystems, Waltham, MA). The relative abundance of specific mRNAs was normalized to human glyceraldehyde 3-phosphate dehydrogenase (GAPDH) mRNA as the internal control. The qPCR primer sequences were as follows:

KIF7(F): AACGGCTCTGTGGTCAGC.

KIF7(R): AGCACCTTCTCCATCTCCTG.

SCLT1(F): AGAGAACTGTGGGCTTGTCA.

SCLT1(R): CTCCAGGGCAATCTTCCTTA.

IFT43(F): AGATTTGGGGCTGGCTTC.

IFT43(R): CAGGTCACGGTAGGTCATCA.

RNF38(F): ATCTCCCTTACGCACAGCAG.

RNF38(R): TGGATGAGCAGCAGGATGTA.

TOPORS(F): GATTGCCCTGCTCCTTCATA.

TOPORS(R): TGGTGCCTGACTAACAGTGG.

C5orf30(F): ATTTGGTTGGCTTCACGACT.

C5orf30(R): GGCTTCTGCTTTGCTCTCTT.

GAPDH(F): AAGGTCGGAGTCAACGGATTTG.

GAPDH(R): CCATGGGTGGAATCATATTGGAA.

Western blotting

Cells were lysed using the CelLytic ^{TM} M cell lysis reagent (Sigma, St. Louis, MO) with protease cocktail inhibitors (Roche, Mannhein, Germany) on ice for 10 minutes. Next, the lysates were centrifuged at 13,300 rpm for 10 minutes at 4 °C. The cell lysates were collected and quantified using the Bradford protein quantity assay (Bio–Rad, Hercules, CA, USA). The quantified lysates were mixed with sample buffer and heated at 100 °C for 20 minutes. Next, the prepared samples were loaded on gels and separated by SDS–PAGE. After gel separation, the samples were transferred to PVDF membranes at 20 V for 720 min in a cold room. After washing with TBST, the membranes were blocked with 3% BSA in TBST at room temperature for 1 hour. Next, the membranes were incubated with primary antibodies at 4 °C for 12 hours. Following extensive washing with TBST three times, the membranes were incubated with HRP-conjugated secondary antibodies at room temperature for 1 hour. After washing with TBST three times, the signals were detected by ECL™ Detection Reagents.

Statistical analysis

All the results were presented as means ± S.D. from at least three independent experiments, and more than 500 cells were counted in each individual group. The error bars in bar plots represent the standard error of the mean from at least three independent experiments. Differences between two groups were compared using unpaired two-tailed *t*-tests and ANOVA for multigroup comparisons, for which a P value < 0.05 was considered statistically significant.

Abbreviations

ATM, ataxia telangiectasia mutated

ATR, ATM-Rad3-related

ARL13b, ADP ribosylation factor-like GTPases 13b

AMPK, AMP-activated protein kinase

ATG7, autophagy related 7

AZI1, azacytidine-inducible-1

ac-tub, acetylated tubulin

AKT, Protein kinase B, PKB

BBS4, Bardet-Biedl syndrome 4

BafA1, Bafilomycin A1

CPT, cisplatin

C5orf30, chromosome 5 open reading frame 30

CEP164, centrosomal protein 164

CEP131, centrosomal protein 131

CEP290, centrosomal protein 290

CP110, centriolar coiled coil protein 110

CHEK1, checkpoint kinase 1

CHEK2, checkpoint kinase 2

CQ, chloroquine

DNA-PK, DNA-dependent protein kinase

EFoCS, excessive formation of centriolar satellites

ETO, etoposide

FBS, fetal bovine serum

GEM, gemcitabine

GAPDH, glyceraldehyde 3-phosphate dehydrogenase

HU, 5-Fluorouracil

IFT88, intraflagellar transport 88

IFT43, intraflagellar transport 43

KIF7, kinesin family member 7

LC3, light chain 3

NF-κB, nuclear factor kappa B

OFD1, oral-facial-digital syndrome 1

PanIN, pancreatic intraepithelial neoplasia

PDAC, pancreatic ductal adenocarcinoma

PI3KK, phosphatidylinositol 3-kinase-related protein kinase

PCM1, pericentriolar material 1

PARP, poly (ADP-Ribose) polymerase

RPMI-1640, Roswell Park Memorial Institute 1640

RNF38, ring finger protein 38

Rosco, roscovitine

SCLT1, sodium channel and clathrin linker 1

SOV, sodium orthovanadate

ULK1, UNC-51-like kinase-1

taxol, paclitaxel

TOPORS, TOP1 binding arginine/serine rich protein, E3 Ubiquitin Ligase

Declarations

Competing interests

The authors declare that they have no competing interests.

Funding

This study was supported by grants from the Ministry of Science and Technology of Taiwan.

MOST109-2320-B-006-042-MY3 and MOST109-2320-B-006-034 to Chia-Yih Wang.

MOST109-2320-B-006-035 to Shaw-Jenq Tsai.

MOST109-2320-B-006-037 to Wen-Tai Chiu.

MOST109-2320-B-006-036 to Pai-Sheng Chen.

Authors' contributions

Conceptualization: B.-M. H., C.-Y. W., and S.-J. T.; Methodology: Y.-Y. C., I-C. P., P.-R. L., Y.-S. L., and J.-H. C.; Investigation: Y.-Y. C., W.-T. C., Y.-S. L., S.-C. L., and P.-S. C.; Software and formal analysis: Y.-Y. C., Y.-S. L., and W.-T. C.; Writing, Review, and Editing: B.-M. H., C.-Y. W., and S.-J. T.; Supervision and funding acquisition: W.-T. C., P.-S. C., C.-Y. W., and S.-J. T. The authors read and approved the final manuscript.

Acknowledgements

1. We thank the National RNAi Core Facility at Academia Sinica in Taiwan for providing shRNA reagents and related services.

2 We are grateful for the support from the Core Research Laboratory, College of Medicine, National Cheng Kung University.

3. This study was supported by grants from the Ministry of Science and Technology (MOST109-2320-B-006-042-MY3 and MOST109-2320-B-006-034 to Chia-Yih Wang; MOST109-2320-B-006-035 to Shaw-Jenq Tsai; MOST109-2320-B-006-037 to Wen-Tai Chiu; MOST109-2320-B-006-036 to Pai-Sheng Chen.)

References

1. Kuehn BM: **Looking to Long-term Survivors for Improved Pancreatic Cancer Treatment.** *JAMA* 2020, **324:**2242-2244.
2. Sung H, Ferlay J, Siegel RL, Laversanne M, Soerjomataram I, Jemal A, Bray F: **Global Cancer Statistics 2020: GLOBOCAN Estimates of Incidence and Mortality Worldwide for 36 Cancers in 185 Countries.** *CA Cancer J Clin* 2021, **71:**209-249.
3. Zeng S, Pottler M, Lan B, Grutzmann R, Pilarsky C, Yang H: **Chemoresistance in Pancreatic Cancer.** *Int J Mol Sci* 2019, **20**.
4. Lord CJ, Ashworth A: **The DNA damage response and cancer therapy.** *Nature* 2012, **481:**287-294.
5. Woods D, Turchi JJ: **Chemotherapy induced DNA damage response: convergence of drugs and pathways.** *Cancer Biol Ther* 2013, **14:**379-389.
6. Cremona CA, Behrens A: **ATM signalling and cancer.** *Oncogene* 2014, **33:**3351-3360.
7. Kwok M, Davies N, Agathanggelou A, Smith E, Oldreive C, Petermann E, Stewart G, Brown J, Lau A, Pratt G, et al: **ATR inhibition induces synthetic lethality and overcomes chemoresistance in TP53- or ATM-defective chronic lymphocytic leukemia cells.** *Blood* 2016, **127:**582-595.
8. Shi Q, Shen LY, Dong B, Fu H, Kang XZ, Yang YB, Dai L, Yan WP, Xiong HC, Liang Z, Chen KN: **The identification of the ATR inhibitor VE-822 as a therapeutic strategy for enhancing cisplatin chemosensitivity in esophageal squamous cell carcinoma.** *Cancer Lett* 2018, **432:**56-68.
9. Liu J, Liu Y, Meng L, Ji B, Yang D: **Synergistic Antitumor Effect of Sorafenib in Combination with ATM Inhibitor in Hepatocellular Carcinoma Cells.** *Int J Med Sci* 2017, **14:**523-529.
10. Corbit KC, Aanstad P, Singla V, Norman AR, Stainier DY, Reiter JF: **Vertebrate Smoothened functions at the primary cilium.** *Nature* 2005, **437:**1018-1021.
11. Nusse R: **Wnts and Hedgehogs: lipid-modified proteins and similarities in signaling mechanisms at the cell surface.** *Development* 2003, **130:**5297-5305.
12. Pazour GJ, Witman GB: **The vertebrate primary cilium is a sensory organelle.** *Curr Opin Cell Biol* 2003, **15:**105-110.

13. Singla V, Reiter JF: **The primary cilium as the cell's antenna: signaling at a sensory organelle.** *Science* 2006, **313:**629-633.
14. Seeley ES, Carriere C, Goetze T, Longnecker DS, Korc M: **Pancreatic cancer and precursor pancreatic intraepithelial neoplasia lesions are devoid of primary cilia.** *Cancer Res* 2009, **69:**422-430.
15. Menzl I, Lebeau L, Pandey R, Hassounah NB, Li FW, Nagle R, Weihs K, McDermott KM: **Loss of primary cilia occurs early in breast cancer development.** *Cilia* 2014, **3:**7.
16. Deng YZ, Cai Z, Shi S, Jiang H, Shang YR, Ma N, Wang JJ, Guan DX, Chen TW, Rong YF, et al: **Cilia loss sensitizes cells to transformation by activating the mevalonate pathway.** *J Exp Med* 2018, **215:**177-195.
17. Jenks AD, Vyse S, Wong JP, Kostaras E, Keller D, Burgoyne T, Shoemark A, Tsalikis A, de la Roche M, Michaelis M, et al: **Primary Cilia Mediate Diverse Kinase Inhibitor Resistance Mechanisms in Cancer.** *Cell Rep* 2018, **23:**3042-3055.
18. Odabasi E, Batman U, Firat-Karalar EN: **Unraveling the mysteries of centriolar satellites: time to rewrite the textbooks about the centrosome/cilium complex.** *Mol Biol Cell* 2020, **31:**866-872.
19. Odabasi E, Gul S, Kavakli IH, Firat-Karalar EN: **Centriolar satellites are required for efficient ciliogenesis and ciliary content regulation.** *EMBO Rep* 2019, **20**.
20. Loffler H, Fechter A, Liu FY, Poppelreuther S, Kramer A: **DNA damage-induced centrosome amplification occurs via excessive formation of centriolar satellites.** *Oncogene* 2013, **32:**2963-2972.
21. Villumsen BH, Danielsen JR, Povlsen L, Sylvestersen KB, Merdes A, Beli P, Yang YG, Choudhary C, Nielsen ML, Mailand N, Bekker-Jensen S: **A new cellular stress response that triggers centriolar satellite reorganization and ciliogenesis.** *EMBO J* 2013, **32:**3029-3040.
22. Kurtulmus B, Wang W, Ruppert T, Neuner A, Cerikan B, Viol L, Duenas-Sanchez R, Gruss OJ, Pereira G: **WDR8 is a centriolar satellite and centriole-associated protein that promotes ciliary vesicle docking during ciliogenesis.** *J Cell Sci* 2016, **129:**621-636.
23. Sui X, Chen R, Wang Z, Huang Z, Kong N, Zhang M, Han W, Lou F, Yang J, Zhang Q, et al: **Autophagy and chemotherapy resistance: a promising therapeutic target for cancer treatment.** *Cell Death Dis* 2013, **4:**e838.
24. Egan DF, Shackelford DB, Mihaylova MM, Gelino S, Kohnz RA, Mair W, Vasquez DS, Joshi A, Gwinn DM, Taylor R, et al: **Phosphorylation of ULK1 (hATG1) by AMP-activated protein kinase connects energy sensing to mitophagy.** *Science* 2011, **331:**456-461.
25. Tanida I, Ueno T, Kominami E: **LC3 and Autophagy.** *Methods Mol Biol* 2008, **445:**77-88.
26. Husson H, Moreno S, Smith LA, Smith MM, Russo RJ, Pitstick R, Sergeev M, Ledbetter SR, Bukanov NO, Lane M, et al: **Reduction of ciliary length through pharmacologic or genetic inhibition of CDK5 attenuates polycystic kidney disease in a model of nephronophthisis.** *Hum Mol Genet* 2016, **25:**2245-2255.
27. Goetz SC, Liem KF, Jr., Anderson KV: **The spinocerebellar ataxia-associated gene Tau tubulin kinase 2 controls the initiation of ciliogenesis.** *Cell* 2012, **151:**847-858.

28. Kodani A, Tonthat V, Wu B, Sutterlin C: **Par6 alpha interacts with the dynactin subunit p150 Glued and is a critical regulator of centrosomal protein recruitment.** *Mol Biol Cell* 2010, **21:**3376-3385.
29. Chen TY, Huang BM, Tang TK, Chao YY, Xiao XY, Lee PR, Yang LY, Wang CY: **Genotoxic stress-activated DNA-PK-p53 cascade and autophagy cooperatively induce ciliogenesis to maintain the DNA damage response.** *Cell Death Differ* 2021, **28:**1865-1879.
30. Pampliega O, Orhon I, Patel B, Sridhar S, Diaz-Carretero A, Beau I, Codogno P, Satir BH, Satir P, Cuervo AM: **Functional interaction between autophagy and ciliogenesis.** *Nature* 2013, **502:**194-200.
31. Ding XF, Zhou J, Hu QY, Liu SC, Chen G: **The tumor suppressor pVHL down-regulates never-in-mitosis A-related kinase 8 via hypoxia-inducible factors to maintain cilia in human renal cancer cells.** *J Biol Chem* 2015, **290:**1389-1394.
32. Rocha C, Papon L, Cacheux W, Marques Sousa P, Lascano V, Tort O, Giordano T, Vacher S, Lemmers B, Mariani P, et al: **Tubulin glycylases are required for primary cilia, control of cell proliferation and tumor development in colon.** *EMBO J* 2014, **33:**2247-2260.
33. Guen VJ, Chavarria TE, Kroger C, Ye X, Weinberg RA, Lees JA: **EMT programs promote basal mammary stem cell and tumor-initiating cell stemness by inducing primary ciliogenesis and Hedgehog signaling.** *Proc Natl Acad Sci U S A* 2017, **114:**E10532-E10539.
34. Kim H, Xu H, George E, Hallberg D, Kumar S, Jagannathan V, Medvedev S, Kinose Y, Devins K, Verma P, et al: **Combining PARP with ATR inhibition overcomes PARP inhibitor and platinum resistance in ovarian cancer models.** *Nat Commun* 2020, **11:**3726.
35. Marechal A, Zou L: **DNA damage sensing by the ATM and ATR kinases.** *Cold Spring Harb Perspect Biol* 2013, **5**.
36. Salunkhe S, Mishra SV, Nair J, Ghosh S, Choudhary N, Kaur E, Shah S, Patkar K, Anand D, Khattry N, et al: **Inhibition of novel GCN5-ATM axis restricts the onset of acquired drug resistance in leukemia.** *Int J Cancer* 2018, **142:**2175-2185.
37. Gomes LR, Rocha CRR, Martins DJ, Fiore A, Kinker GS, Bruni-Cardoso A, Menck CFM: **ATR mediates cisplatin resistance in 3D-cultured breast cancer cells via translesion DNA synthesis modulation.** *Cell Death Dis* 2019, **10:**459.
38. Tang Z, Lin MG, Stowe TR, Chen S, Zhu M, Stearns T, Franco B, Zhong Q: **Autophagy promotes primary ciliogenesis by removing OFD1 from centriolar satellites.** *Nature* 2013, **502:**254-257.
39. Chen TY, Lin TC, Kuo PL, Chen ZR, Cheng HL, Chao YY, Syu JS, Lu FI, Wang CY: **Septin 7 is a centrosomal protein that ensures S phase entry and microtubule nucleation by maintaining the abundance of p150(glued).** *J Cell Physiol* 2021, **236:**2706-2724.
40. Delaval B, Bright A, Lawson ND, Doxsey S: **The cilia protein IFT88 is required for spindle orientation in mitosis.** *Nat Cell Biol* 2011, **13:**461-468.
41. Graser S, Stierhof YD, Lavoie SB, Gassner OS, Lamla S, Le Clech M, Nigg EA: **Cep164, a novel centriole appendage protein required for primary cilium formation.** *J Cell Biol* 2007, **179:**321-330.
42. Hori A, Barnouin K, Snijders AP, Toda T: **A non-canonical function of Plk4 in centriolar satellite integrity and ciliogenesis through PCM1 phosphorylation.** *EMBO Rep* 2016, **17:**326-337.

43. Delgehyr N, Sillibourne J, Bornens M: **Microtubule nucleation and anchoring at the centrosome are independent processes linked by ninein function.** *J Cell Sci* 2005, **118:**1565-1575.
44. Andreassen PR, D'Andrea AD, Taniguchi T: **ATR couples FANCD2 monoubiquitination to the DNA-damage response.** *Genes Dev* 2004, **18:**1958-1963.
45. An J, Yang DY, Xu QZ, Zhang SM, Huo YY, Shang ZF, Wang Y, Wu DC, Zhou PK: **DNA-dependent protein kinase catalytic subunit modulates the stability of c-Myc oncoprotein.** *Mol Cancer* 2008, **7:**32.
46. Kramer A, Mailand N, Lukas C, Syljuasen RG, Wilkinson CJ, Nigg EA, Bartek J, Lukas J: **Centrosome-associated Chk1 prevents premature activation of cyclin-B-Cdk1 kinase.** *Nat Cell Biol* 2004, **6:**884-891.

Figures

Figure 1

Cisplatin induces primary cilia formation in PDAC. (A-B) Chemotherapeutic drugs induce primary cilia formation. (A) Primary cilia were detected by immunostaining using an antibody against ARL13b in control (CTL) or cisplatin (CPT)-treated PANC-1 cells. Arrows indicate primary cilia. Scale bar, 20 μm. (B) Quantitative results of the frequency of ciliated cells in the absence (CTL) or presence of cisplatin (CPT; 5 μM; 72 h), gemcitabine (GEM; 100 μM; 72 h), etoposide (ETO; 100 μM; 48 h), or paclitaxel (Taxol; 0.1 μg/ml; 24 h). (C-E) CPT-induced primary cilia grew in a dose- and time-dependent manner. Quantitative results of the frequency of ciliated cells after treatment with different concentrations (0, 1, 2.5, or 5 μM) of CPT for (C) 24 h, (D) 48 h, or (E) 72 h. (F) Tubulin acetylation increased following CPT treatment. Extracts of PANC-1 cells treated with or without CPT were analyzed by immunoblotting with antibodies against acetylated tubulin (Ac-tub) and tubulin. (G-I) CPT induced primary cilia formation in PANC-1 cells. Double staining of CPT-treated cells with antibodies against (G) acetylated tubulin (Ac-tub) and CEP164, (H) ARL13b, or (I) IFT88. DNA was stained with DAPI (blue). Scale bar, 10 μm. (J) PANC-1 cells grew primary cilia in a density-dependent manner. Quantitative results of the frequency of ciliated cells in different densities of PANC-1 cells. (K) CPT-resistant PNAC-1 cells grew primary cilia. Quantitative results of the frequency of ciliated cells in wild-type (WT) or CPT-resistant (CPT Resist) PANC-1 cells. n.s. no significance, * $P<0.05$, ** $P<0.01$, *** $P<0.001$.

Figure 2

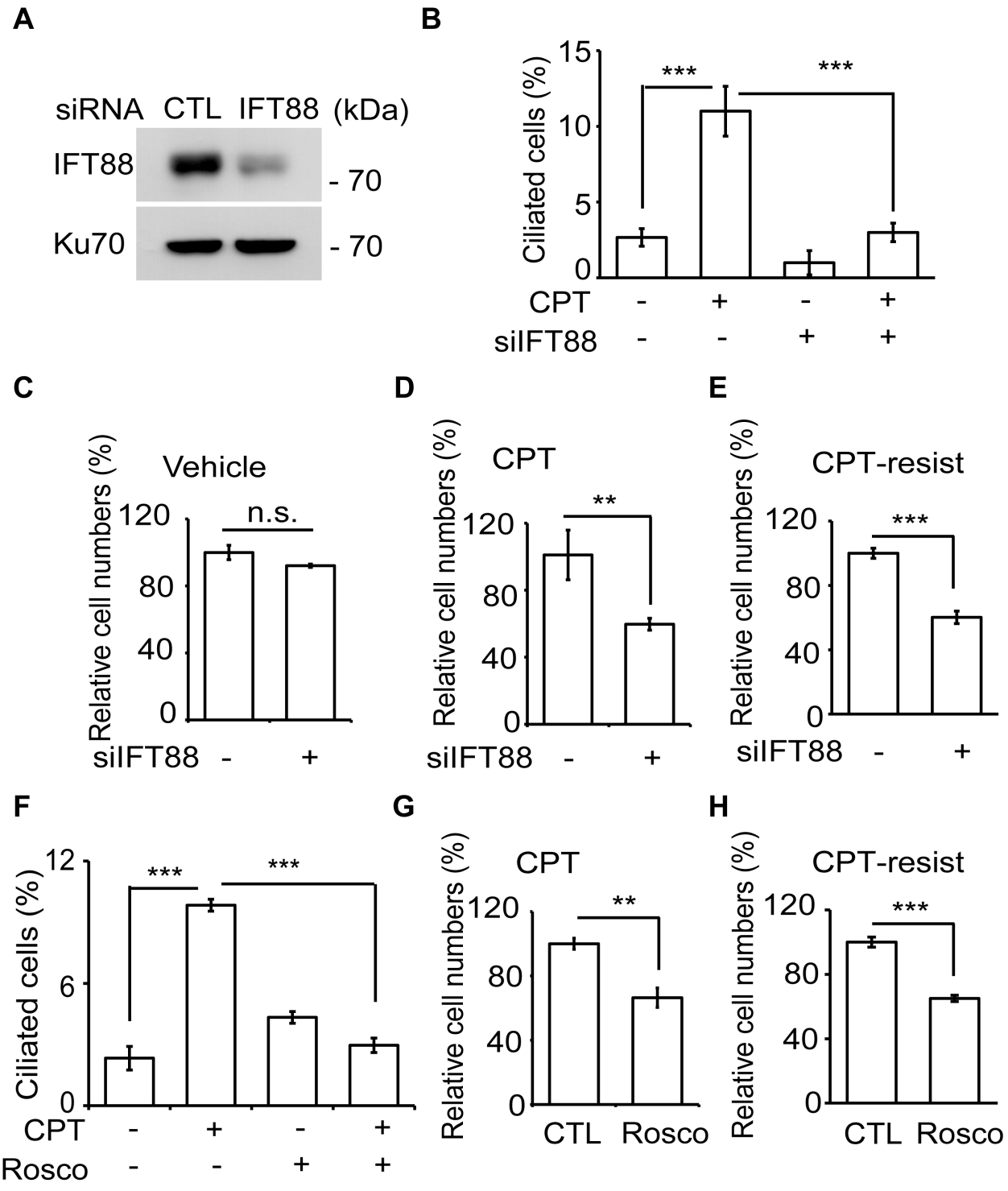

Figure 2

Primary cilia contribute to chemoresistance in PANC-1 cells. (A-E) IFT88 depletion inhibited primary ciliogenesis and cell viability. (A) IFT88 was efficiently depleted. Extracts of cells transfected with siRNA against IFT88 (siIFT88) were analyzed by immunoblotting with antibodies against IFT88 and Ku70. (B) Reduced ciliogenesis in IFT88-deficient cells. Quantitative results of the frequency of ciliated control and IFT88-deficient PANC-1 cells in the absence or presence of cisplatin (CPT). (C-D) Depletion of IFT88

reduced cell viability following CPT treatment. Quantitative results of the relative cell numbers in control and IFT88-deficient PANC-1 cells in the absence (C) or presence (D) of CPT. (E) Depletion of IFT88 decreased cell viability in CPT-resistant PANC-1 cells. Quantitative results of the relative cell numbers in control or IFT88-depleted CPT-resistant (CPT-resist) PANC-1 cells. (F-G) Roscovitine (Rosco) inhibited primary cilia efficiently and sensitized cells to CPT treatment. Quantitative results of the frequency of ciliated cells (F) and relative cell number (G) after treatment with CPT in the presence or absence of roscovitine (Rosco, 20 μM) for 72 h. (H) Roscovitine reduced cell viability in CPT-resistant (CPT-resist) PANC-1 cells. Quantitative results of the relative cell numbers in CPT-resistant PANC-1 cells treated with Rosco (20 μM). n.s. no significance, ** P<0.01, *** P<0.001.

Figure 3

Excessive formation of centriolar satellites (EFoCS) contributes to primary ciliogenesis and chemoresistance. (A-B) EFoCS was observed in CPT-treated PANC-1 cells. (A) EFoSCs were visualized by immunostaining with antibodies against γ-tubulin (γ-tub) and PCM1. DNA was stained with DAPI (blue). Scale bar, 10 μm. (B) Quantitative results of the cells with EFoCS following CPT treatment. (C) The amounts of PCM1 were upregulated following CPT treatment. Extracts of CPT-treated PANC-1 cells were analyzed by immunoblotting with antibodies against PCM1 and Ku70. (D-E) PCM1 depletion inhibited CPT-induced primary ciliogenesis. (D) PCM1 was efficiently depleted by transfecting cells with siRNA against PCM1 (siPCM1). Extracts of siPCM1-transfected cells were analyzed by immunoblotting with antibodies against PCM1 and Ku70. (E) Quantitative results of the frequency of ciliated control and PCM1-deficient PANC-1 cells in the absence or presence of CPT. (F-G) PCM1 depletion sensitized cells to CPT treatment. Quantitative results of the relative cell numbers in control and PCM1-deficient PANC-1 cells in the absence (F) or presence (G) of CPT. (H) PCM1 depletion reduced cell viability in CPT-resistant (CPT-resist) PANC-1 cells. Quantitative results of the relative cell numbers of control (CTL) or PCM1-depleted CPT-resistant PANC-1 cells. (I-K) Disruption of EFoCS alleviated primary ciliogenesis. (I) p150glued was depleted efficiently. Extracts of cells transfected with siRNA against p150glued (sip150) were analyzed by immunoblotting with antibodies against p150 and Ku70. (J) Depletion of p150glued disrupted EFoCS efficiently, as shown by immunostaining with antibodies against γ-tubulin (γ-tub) and PCM1. DNA was stained with DAPI (blue). Scale bar, 10 μm. (K) Quantitative results of the frequency of ciliated control or p150-deficient PANC-1 cells in the absence or presence of CPT. * P<0.05, ** P<0.01, *** P<0.001.

Figure 4

ATM and ATR contribute to CPT chemoresistance in pancreatic cancer. (A) CPT induced DNA damage in PANC-1 cells. DNA damage was examined by immunostaining using an antibody against γ-H2AX (green) in control (CTL) or cisplatin (CPT)-treated PANC-1 cells. DNA was stained with DAPI (blue). Scale bar, 20 μm. (B) DNA damage signaling was activated under CPT treatment. Extracts of CPT-treated PANC-1 cells

were analyzed by immunoblotting with antibodies against phosphorylated ATM (p-ATM), ATM, phosphorylated ATR (p-ATR), ATR, phosphorylated DNA-PKcs (p-PKcs), DNA-PKcs (PKcs), and Ku70. (C-F) ATM and ATR participated in CPT-induced ciliogenesis. (C and E) ATM and ATR were depleted efficiently by siRNA transfection. Extracts of cells transfected with siRNA against (C) ATM or (E) ATR were analyzed by immunoblotting with antibodies against ATM, ATR, and Ku70. (D and F) Quantitative results of ciliated cells in the presence or absence of CPT in cells treated with siRNA against (D) ATM or (F) ATR. (G-J) ATM and ATR maintained cell viability following CPT treatment. Quantitative results of the relative cell numbers of PANC-1 cells treated with siRNA against ATM (G-H) or ATR (I-J) in the absence (vehicle, G and I) or presence of CPT (H and J). (K) The depletion of ATM or ATR reduced cell viability in CPT-resistant PANC-1 cells. Quantitative results of the relative cell numbers in siATM- or siATR-transfected CPT-resistant (CPT-resist) PANC-1 cells. n.s. no significance, * P<0.05, ** P<0.01, *** P<0.001.

Figure 5

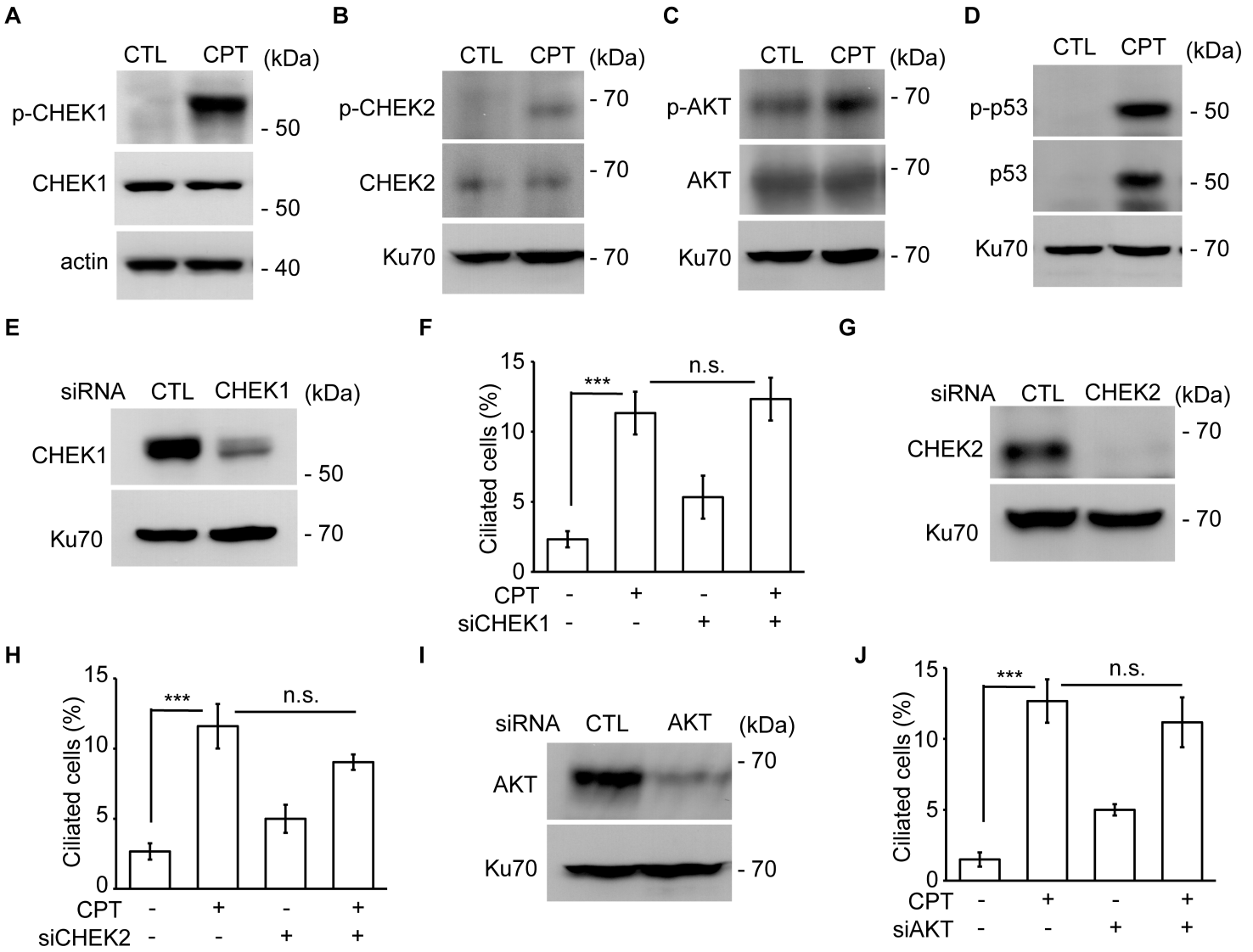

Figure 5

Activation of CHEK1, CHEK2, AKT, or p53 does not contribute to CPT-induced primary ciliogenesis. (A-D) The downstream effectors of DNA damage, including (A) CHEK1, (B) CHEK2, (C) AKT, and (D) p53, were activated following CPT treatment. Extracts of CPT-treated PANC-1 cells were analyzed by immunoblotting with antibodies against phosphorylated CHEK1 (p-CHEK1), CHEK1, phosphorylated CHEK2 (p-CHEK2), CHEK2, phosphorylated AKT (p-AKT), AKT, phosphorylated p53 (p-p53), p53 and Ku70. (E-J) Depletion of CHEK1, CHEK2 or AKT had no effects on CPT-induced primary cilia formation. (E) CHEK1, (G) CHEK2, and (I) AKT were depleted by siRNA transfection. Extracts of cells transfected with or without siRNA were analyzed by immunoblotting with antibodies against CHEK1, CHEK2, AKT and Ku70. Quantitative results of the frequency of ciliated control, (F) CHEK1-, (H) CHEK2-, or (J) AKT-deficient PANC-1 cells in the absence or presence of CPT. n.s. no significance, *** P<0.001.

Figure 6

Autophagy contributes to cisplatin resistance in PANC-1 cells. (A-B) CPT activated autophagy. (A) LC3 puncta were increased in CPT-treated PANC-1 cells, as shown by immunostaining with an antibody against LC3. Scale bar, 10 μm. (B) CPT promoted the conversion of LC3 I to II. Extracts of CPT-treated PANC-1 cells were analyzed by immunoblotting with antibodies against LC3 and actin. (C-D) AMPK and ULK1 were activated by CPT treatment. Extracts of CPT-treated PANC-1 cells were analyzed by immunoblotting with antibodies against phosphorylated AMPK (at Thr 172, active phosphorylation), AMPK, phosphorylated ULK1 (at Ser 757, inhibitory phosphorylation), ULK1, and Ku70. (E-F) Depletion of ATG7 reduced CPT-induced ciliogenesis and cell viability. (E) ATG7 was depleted by infecting cells with lentivirus containing different shRNA sequences (#1–3) against ATG7. Extracts of PANC-1 cells infected with lentivirus containing shATG7#1–3 and shLuc (control) were analyzed by immunoblotting with antibodies against ATG7 and actin. (F) Depletion of ATG7 inhibited primary ciliogenesis. Quantitative results of the proportion of cells with primary cilia in ATG7-depleted (#3) cells in the presence or absence of CPT. (G-H) Depletion of ATG7 reduced cell viability following CPT treatment. Quantitative results of the relative cell numbers in vehicle control (G) or CPT-treated (H) PANC-1 cells. (I) Inhibition of AMPK or ULK1 reduced cell viability in CPT-resistant PANC-1 cells. Quantitative results of the relative cell numbers in the absence or presence of AMPK inhibitor (AMPKi, 5 μM) or ULK1 inhibitor (ULK1i; 10 μM) in CPT-resistant PANC-1 cells. n.s. no significance, *** P<0.001.

Figure 7

ATM and ATR trigger autophagy and excessive formation of centriolar satellites (EFoCS). (A-B) Depletion of ATM or ATR inhibited autophagy. CPT-induced AMPK (A-B, upper panel) or ULK1 (A-B, lower panel) activation was inhibited following ATM (A) or ATR (B) depletion. Extracts of CPT-treated cells transfected with siRNA against ATM (siATM, A) or ATR (siATR, B) were analyzed by immunoblotting with antibodies against phosphorylated ATM (p-ATM), phosphorylated ATR (p-ATR), phosphorylated AMPK (p-AMPK), AMPK and Ku70. (C-D) Depletion of ATM or ATR inhibited EFoCS. (C) EFoCS was examined by

immunostaining with antibodies against γ-tubulin (γ-tub) and PCM1 in ATM- or ATR-deficient cells following CPT treatment. DNA was stained with DAPI (blue). Scale bar, 10 μm. (D) Quantitative results of the ATM- or ATR-deficient cells with EFoCS in the absence or presence of CPT. (E) Depletion of ATM or ATR reduced the expression of CPT-increased PCM1. Extracts of cells transfected with siATM or siATR in the absence or presence of CPT were analyzed by immunoblotting with antibodies against PCM1 and Ku70. (F) ATM and ATR paninhibitor (caffeine) decreased the levels of PCM1. Extracts of cells with caffeine treatment in the absence or presence of CPT were analyzed by immunoblotting with antibodies against PCM1 and Ku70.

Supplementary Files

This is a list of supplementary files associated with this preprint. Click to download.

- SupplementaryfiguresGB.docx
- supplementaryvedio1control.mp4
- supplementaryvedio2CPTtreatment.mp4